

RAPID COMMUNICATION

Plasma generation in a gap around a sliding contact

Keiji Nakayama¹ and Roman A Nevshupa²

National Institute of Advanced Industrial Science and Technology, Namiki 1-2-1, Tsukuba 305-8564, Japan

E-mail: k.nakayama@aist.go.jp and nevshupa@mt11.bmstu.ru

Received 24 January 2002

Published 31 May 2002

Online at stacks.iop.org/JPhysD/35/L53**Abstract**

It has been hypothesized that plasma is generated at a sliding contact. However, it has not yet been found. Here, we report on a discovery of plasma generated in the microscopic gap around a sliding contact, having an elliptical shape with a horseshoe pattern and with a size beyond a hundred micrometers. It emits mostly invisible ultraviolet (UV) photons and, to a lesser extent, infrared (IR) photons. It must be a main source of the curious tribophysical and chemical phenomena. The origin, characteristics and the relation to these curious phenomena are discussed.

A hypothesis of plasma generation at a sliding contact was first proposed in 1965 [1]. For more than a quarter of a century since then, almost no essential work on tribo-plasma generation has been reported. Recently, Nakayama has succeeded in measuring the triboemission, i.e. emission of charged particles at a sliding contact, under various conditions using specially developed apparatuses [1–10]. The triboemission of electrons, ions and photons was observed in ambient air [1–3], in various gases [4–6] and in liquids [7] for insulators [4–7], semiconductors [2, 3, 7], and oxide-covered metals [3], even in the simulation system of a head sliding on a magnetic recording disk in a hard disk drive (HDD) [8, 9]. It was found that the intensity of particle emission was a function of the *electrical* resistivity of sliding solids [10], i.e. it is related to the tribocharging. The same numbers of negatively and positively charged particles were detected emitting from a sliding contact [3, 10]. Based on these results, Nakayama proposed a new discharge plasma model [11], since plasma is defined as a state where the same numbers of free negatively and positively charged particles coexist to give a neutral state [12]. This model is different from the magma-plasma model proposed in 1965 in which electrons and photons are emitted from the magma-plasma state of materials produced in the sub-microscopic region of the sliding contact. This discharge

model suggests that the emission of electrons, ions and photons occurs from microscopic plasma, i.e. microplasma, which is formed in the gap of the sliding contact due to the discharging of ambient gas in the electric field generated by frictional electrification. Frictional electrification is the generation of static electrical charges by rubbing one material against another.

The concept of microplasma is very promising, to help solve the various serious tribophysical and tribochemical problems, such as the dissipation mechanism of tribocharge and the tribochemical decomposition mechanism of lubricants like the thin perfluoropolyether (PFPE) film coating on magnetic recording disk in HDD [13]. Several mechanisms of tribocharging have been proposed [14], but the dissipation mechanism is obscure. Therefore, microplasma can be a good candidate for the tribocharge dissipation process. Concerning tribochemical problems, the traditional thermal effects or catalytic actions do not explain completely the tribochemical reactions. Very recently, much attention is being denoted to tribo-microplasma as the most plausible candidate for the origin of the tribochemical reactions [11]. So, it was reported that n-butane gas molecules were decomposed intensively at the sliding contact in the condition under which triboemission intensity reached maximum [6]. However, no successful direct observation of the existence of the tribo-microplasma has been obtained. The discovery of tribo-microplasma generation will open up a new field of tribophysics and tribochemistry and

¹ Author to whom correspondence should be addressed.

² On leave from Bauman Moscow State Technical University. Permanent address: BMSTU, MT-11, 2-Baumanskaia 5, Moscow 107005, Russia.

solve the various tribology related problems in our daily life and in industry.

Since tribo-plasma emits photons in ambient air, we can verify the existence of the plasma by measuring the two-dimensional image of photon emissions from the sliding contact. From the image we can determine the location, overall shape and intensity distribution of the tribo-microplasma. Figures 1(a) and (b) show the apparatuses to measure the image of the photon emissions from a pin-on-disk sliding contact from the sideview (figure 1(a)) and backview through the disk (figure 1(b)). Both apparatuses were composed of an optical microscope with a quartz lens system, a filter, an intensified charge coupled device (ICCD) and a personal computer (PC). Hemispherical diamond pins had radii $r = 300$ and $500 \mu\text{m}$, respectively, while disks were made of sapphire with a thickness of 1 mm and a photon transmission range from 180 to 4500 nm and of soda-lime glass. The glass disk was a substrate of the magnetic recording disk. The experiments were conducted at a normal force $F_N = 30\text{--}834$ mN and a sliding velocity $V = 2.0\text{--}145$ cm s⁻¹ in ambient air with relative humidity (RH) 30–40% at room temperature. The specimens were thoroughly cleaned and then dried in a hot air stream. Photon images were obtained at exposure times of 6, 60 and 300 s without filters and also with UV and IR filters, which have transmission ranges $\lambda = 290\text{--}420$ nm and $\lambda = 720\text{--}2800$ nm, respectively.

Figures 1(c)–(e) show the two-dimensional images of photon emission from the sideview without a filter, with UV and with IR filters, respectively. The total image without a filter was combined with an optical micrographic image of the pin-and-disk contact under lighting. It clearly shows that the photon emission occurs in the microscopic gap around the contact. As the optical axis of the microscope was inclined to the plane of the disk surface at a small angle, the images of the diamond tip and emitted photons were reflected on the disk surface to give their mirror images. Strong UV and weak but definite IR images were also clearly detected as shown in figures 1(d) and (e), respectively. All the three kinds of images completely overlapped. According to Nakayama's plasma model, the plasma is formed by electrical discharge of the ambient gas. The spectrum of the triboemitted photons in air was completely consistent with the discharge spectrum of nitrogen gas [15]. Both oxygen and nitrogen gases are ionized through discharging in air, but oxygen discharge does not emit photons [5]; thus, only the nitrogen discharge spectrum was observed. This is because the strength of the electric field generated at the frictional surface was sufficient for nitrogen but insufficient for oxygen to cause sparks, i.e. discharging with photon emission. Thus, it is concluded that the above-observed UV image is a plasma image due to discharging of nitrogen in ambient air. The overlapping of UV and IR images implies that the microplasma also produces a rise in temperature.

Figures 1(f)–(h) show total, UV and IR images measured from the backview through the sapphire disk. A *Hertzian* elastic contact circle [16] with a diameter $d_H = 19 \mu\text{m}$ was depicted together with the experimentally observed contact circle with a diameter $d_{\text{obs}} = 28 \mu\text{m}$. The value of d_H was calculated using the elastic modulus of diamond $E_{\text{dia}} = 1000$ GPa and sapphire $E_{\text{Al}_2\text{O}_3} = 254$ GPa. It should be pointed out that the backview-total images were separated into

two parts: inside and outside of the sliding contact. The photon image outside the contact was broader and more intensive than that inside the contact. In figure 1(g), it was found that the UV image, i.e. plasma image, had a horseshoe pattern surrounding the contact and spreading to the rear. The centre of the plasma horseshoe is located at about $50 \mu\text{m}$ from that of the sliding contact. This is surprising, since for a long time the photons were believed to be emitted from the real sliding contact due to frictional heating [17], or by an extremely intensive high-energy state produced in the deformed layer [1]. From figure 1(h), it was also found that the IR image spreads towards the rear in shape of a ring having the most intensive part at the sliding contact, though the IR intensity was negligible at the centre of the UV horseshoe. The most intensive IR emission, i.e. thermal image, at the sliding contact is reasonable, since strong heat must be produced at the real area of contact by shearing adhesive bonds in the interface. The plasma horseshoe and IR ring completely overlapped. This means that the plasma zone also generates heat. The traditional theory of frictional heating [19] never predicted the observed heat distribution outside the sliding contact. The profile of the surface temperature rise at and around the contact calculated according to the two-dimensional moving heat source theory [18] showed that the maximum temperature is located within the sliding contact, though the point of the maximum temperature lies in the rear half of the contact area. Moreover, the surface temperatures calculated assuming thermal radiation for the UV photons with $\lambda \leq 420$ nm exceeded $34\,000^\circ\text{K}$, which is an unreasonable value for the frictional heating.

Figures 2(a) and (b) show digitally processed contour images of the total photon intensity measured from sideview and backview, respectively, together with the scheme of the contact. The most emission occurs in the gap zone outside the contact. Only weak photon emission occurs at the contact area. This demonstrates that microplasma was neither produced in the sub-microscopic plastic deformed zone at the contact nor originated from the frictional temperature rise. These results contradict the magma-plasma model [1]. The observed distance from the centre of the contact point C to the most intensive discharging point, i.e. the centre of the plasma horseshoe D, was $l_D = 50 \pm 5 \mu\text{m}$, which corresponds to the gap $d_D = 4.6 \pm 0.6 \mu\text{m}$ calculated from the geometry of the contact. *Paschen's* law [20] of electrical gas discharge tells us that the spark voltage, V_s , is a function of the product pd , where p is the gas pressure and d is the separation of parallel electrodes. At the minimum voltage $(V_s)_m$ at $(pd)_m$ gas sparking occurs most easily. The values of $(V_s)_m$ and $(pd)_m$ for air are 330 V and 76 Pa cm, respectively. From the $(pd)_m$ value, the electrode separation at the ambient atmospheric air pressure to initiate sparking was calculated to be $d_{\text{cal}} = 7.5 \mu\text{m}$. The values of $d_D = 4.6 \mu\text{m}$ for frictional contact of a hemisphere on a flat and $d_{\text{cal}} = 7.5 \mu\text{m}$ from Paschen law for parallel plates are surprisingly in good agreement, when we take into account the complicated surface conditions of the frictional dynamic contact, material species, topography and geometry of the two contacting surfaces [20]. Spreading of the microplasma from the point D along the horseshoe to the contact point C, i.e. decreasing the value of the gap means that the generated voltages were beyond

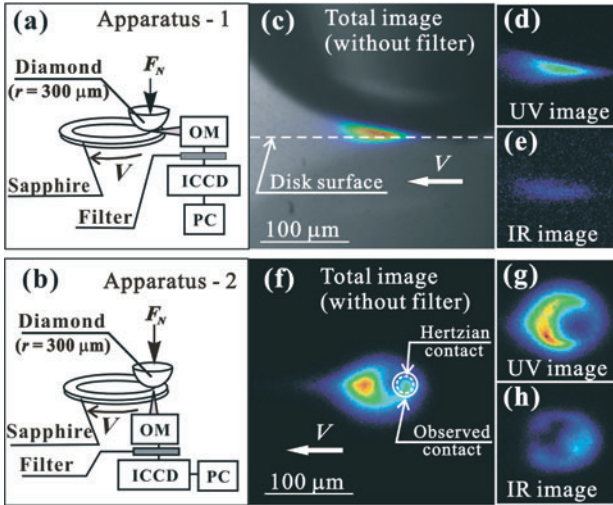


Figure 1. Measuring apparatus from sideview (a) and the backview through the transparent sapphire disk (b). OM: optical microscope; ICCD: intensified charge coupled device; PC: personal computer; (c) combined image of the total emission without filter and optical micrograph of the sliding contact. The horizontal dashed line shows the sapphire disk surface at the contact point; (d) UV image after passing UV transmission filter; (e) IR image after passing the IR transmission filter. The photon intensity was colour scaled in arbitrary units with red indicating 600, 100 and 30 counts of ICCD output in figures 1(c)–(e), respectively. The mirror images reflected on the polished sapphire disk are also accompanied. Figures (f)–(h) show backview images of total, UV and IR emission with red indicating 250, 120 and 120 counts of ICCD output, respectively. Photons are emitted from the microscopic gap around the sliding contact. The emission zone has a size beyond $100\ \mu\text{m}$ and spreads towards the rear. The UV image has an elliptical shape with a pattern of a horseshoe, while IR image has a shape of a ring. The most intensity of the UV emission is outside the contact zone and that of the IR emission is inside the contact zone. The pin radius $r = 300\ \mu\text{m}$ and the disk material was sapphire. Sliding velocity $V = 32.4\ \text{cm s}^{-1}$, the normal force $F_N = 834\ \text{mN}$ and ICCD exposure time $Exp = 6\ \text{s}$.

330 V. It should be pointed out also that the plasma spreads beyond the width of the sliding track. This means that the charge percolation occurs from the friction track outward, e.g. through the adsorbed film.

Figure 3(a) shows the sequential total (top), UV (middle) and IR (bottom) photons images obtained every 20 s after several tens of repeated slidings. It is seen that the patterns of the total and UV plasma images fluctuated with time. This suggests that the distribution of the tribocharge fluctuates with sliding, while temperature-based IR images are rather constant and stable. This might be due to a lower rate of heat dissipation process compared to that of discharging.

Figure 3(b) shows the effect of sliding velocity, V , on the integrated photon emission intensity, N_{ph} , for both UV and IR photons over the photon image. It is seen that the both UV and IR photon intensities increase linearly with the sliding velocity, in which the former intensity was about 8 times higher than the latter. The total UV counts are measured only from one direction from backview and, thus, only a part of the emitted photons are represented. The total photon emission intensity N_{ph} in the present study was 0.4×10^4 – 9.2×10^4 counts per second (cps). For comparison, in a separate works [8, 21], the charged particles emission was measured under

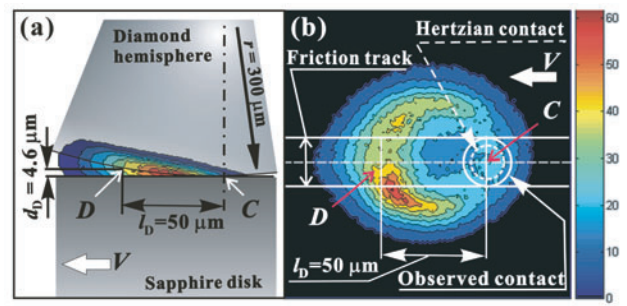


Figure 2. Contour images of the total emission intensity sideview (a) and backview (b), respectively, with the scheme of the contact. The plasma has an elliptical shape with a horseshoe pattern, with the size beyond $100\ \mu\text{m}$, surrounding the contact point and spreading towards the rear. l_D is the distance from the centre of the horseshoe D to the centre of the contact C to the centre of the contact C to the centre of the contact C. Hertzian contact diameter $d_H = 19\ \mu\text{m}$, width of the friction track, i.e. the diameter of observed contact, $d_{\text{obs}} = 28\ \mu\text{m}$. Disk material—sapphire, $V = 32.4\ \text{cm s}^{-1}$, $F_N = 834\ \text{mN}$ and $Exp = 6\ \text{s}$.

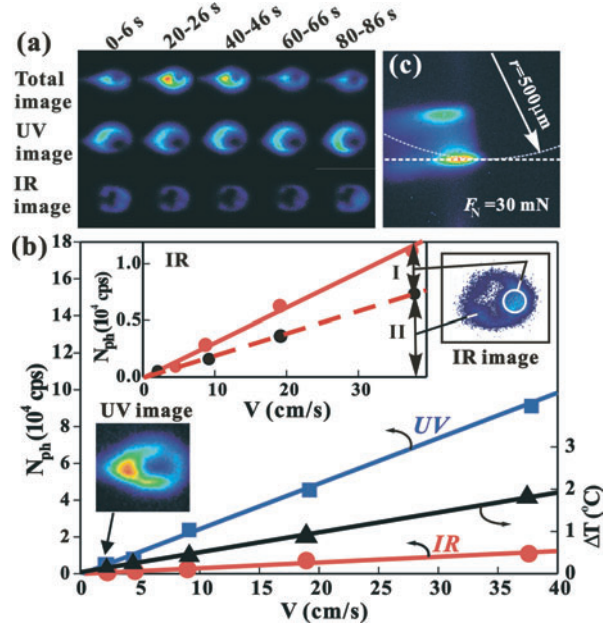


Figure 3. (a) Sequential photon images obtained every 20 s after several tens of revolutions of sliding for total (top), UV (middle) and IR (bottom) images, under $F_N = 30\ \text{mN}$, $V = 32.4\ \text{cm s}^{-1}$ and $Exp = 6\ \text{s}$. Red indicates ICCD output 210, 185 and 185 counts from the top to the bottom. (b) Effect of V on the UV and IR photon emission intensities, N_{ph} , and surface temperature rise, ΔT . Disk material—sapphire, $r = 300\ \mu\text{m}$ and $F_N = 834\ \text{mN}$. The inset shows the dependence of N_{ph} of IR photons on V for the whole area (—) and plasma regions (- - -); (c) total sideview photon image in the HDD simulation tribosystem after 200 s sliding. Disk material—soda-lime glass, $r = 500\ \mu\text{m}$, $F_N = 30\ \text{mN}$, $V = 145\ \text{cm s}^{-1}$ (=500 rpm) and $Exp = 300\ \text{s}$. Red indicates 420 counts of ICCD output. Photons are reflected from both surfaces of pin and disk. Dashed lines show the surfaces of the pin and disk.

similar conditions of a diamond pin ($r = 300\ \mu\text{m}$) sliding on a glass disk with and without hydrogenated amorphous carbon film at $F_N = 840\ \text{mN}$ and $V = 5.8\ \text{cm s}^{-1}$ in ambient air and in Ar gas. It was found that the emission intensity had values $I = 280$ – $350\ \text{pC s}^{-1}$, which corresponds to the

number of charged particles $N_c = 1.8 \times 10^9 - 2.2 \times 10^9$ cps. These values are 5 orders of magnitude higher than that of the photon emission. When we consider that plasma is a mixture of the electrons, negative and positive ions, radicals and excited particles emitting photons, and that oxygen discharge does not emit photons, the entire count of the energetic particles must be much higher than the total counts of the photons and the charged particles measured.

In addition to UV photons, microplasma emits IR photons, which are not originated from frictional heating. The inset of figure 3(b) shows the IR intensities from the total area (solid line) and in the plasma zone (dashed line), i.e. outside of the sliding contact. As it is shown with the arrow (\leftrightarrow) in II, the plasma zone emits roughly 65% of the total IR intensity. Then, the IR emission from the contact zone is less than 5% of the total UV and IR emissions. To check the frictional heating, we calculated surface temperature rise using Archard's theory [19] and Hertzian contact model [16]. As seen in figure 3(b), the calculated temperature rise, ΔT , increases with sliding velocity, V , to the value of 2°C. The temperature rise is negligibly small because of the light sliding conditions and the high thermal conductivity of the diamond tip, while the energetic microplasma was clearly observed even at as low sliding velocity as 2 cm s^{-1} (see UV image in figure 3(b)).

Figure 3(c) shows the total photon image without filter obtained at the sliding contact of a diamond pin with a radius $r = 500 \mu\text{m}$ on a glass substrate of a magnetic recording disk under $F_N = 30 \text{ mN}$ and $V = 500 \text{ rpm}$ (145 cm s^{-1}), which simulates the sliding conditions of a real head on a magnetic recording disk. The microplasma image was definitely detected even at such a low load in the simulation system. The decomposition temperature of the PFPEs used as a lubricant in the HDDs is 190–300°C, while the calculated surface temperature rise was only 0.48°C above the ambient value in this experiment. Frictional thermal reaction as a mechanism of PFPE decomposition should be ruled out now, while a high energetic plasma is a reasonable origin of the tribochemical reactions to cause PFPE decompositions through plasma reactions [22], including photochemical reactions, electron attachment reactions, electron impact reactions, radical reactions and so on. At the moment, the percentage of the frictional energy dissipated through the tribo-microplasma is not determined. The determination of the percentage will be a focus of our future work. However, it is clear that the plasma is essential for the tribochemical reactions.

In this paper, we discovered microplasma generation in a gap of a sliding contact even under as low sliding velocity as 2 cm s^{-1} and as low load as 30 mN. The plasma is almost

invisible and completely different from the well-studied visible and IR photons emission due to frictional heating. It is also different from the well-studied electrostatic discharge phenomena, which occur after complete separation of the tribocharged bodies. The tribo-microplasma discovered in the present paper is generated continuously in the microscopic gap of the sliding contact. The tribo-microplasma explains the mechanisms of the abnormal tribochemical reactions, strange frictional fire accidents [23], and also introduces a new mechanism of energy and tribocharge dissipation under friction. The microplasma also requires a reconstruction of the model of surface temperature distribution over the plasma zone. The discovery of the microplasma opens up a new field of tribo-microplasma science and technology. When we rub almost all materials including insulators, semiconductors and even oxide-covered metals in our daily life and in industry, we are often together with the energetic microplasma without noticing the phenomena.

References

- [1] Thiessen P A 1965 *Z. Chem.* **5** 162
- [2] Nakayama K and Hashimoto H 1991 *Wear* **147** 335
- [3] Nakayama K, Suzuki N and Hashimoto H 1992 *J. Phys. D: Appl. Phys.* **25** 303
- [4] Nakayama K and Hashimoto H 1992 *Tribology Trans.* **35** 643
- [5] Nakayama K and Hashimoto H 1995 *Tribology Trans.* **38** 35
- [6] Nakayama K and Hashimoto H 1996 *Tribology Int.* **29** 385
- [7] Nakayama K and Hashimoto H 1995 *Tribology Trans.* **38** 541
- [8] Nakayama K, Bou-Said B and Ikeda H 1997 *Trans. ASME: J. Tribology* **119** 764
- [9] Nakayama K and Nguyen S 2000 *Appl. Surf. Sci.* **158** 229
- [10] Nakayama K 1999 *Tribology Lett.* **6** 37
- [11] Nakayama K 1997 *J. Japan. Soc. Tribologists* **42** 30 [in Japanese]
- [12] Nagakura S *et al* 1998 *Iwanami Dictionary of Science and Chemistry* (Tokyo: Iwanami-shoten Publishers) p 1191 [in Japanese]
- [13] Novotny V J, Karis T E and Johnson N W 1992 *Trans. ASME: J. Tribology* **114** 61
- [14] Harper W R 1967 *Contact and Frictional Electrification* (Oxford: Clarendon Press) p 23
- [15] Miura T and Nakayama K 2000 *J. Appl. Phys.* **88** 5444
- [16] Hertz H 1881 *J. Reine und Angew. Math.* **92** 56
- [17] Bowden T P and Tabor D 1954 *The Friction and Lubrication of Solids* (Oxford: Clarendon Press)
- [18] Carslaw H S and Jaeger J C 1953 *Conduction of Heat in Solids* (London: Oxford)
- [19] Archard J F 1959 *Wear* **2** 438
- [20] Meek J M and Craggs J D 1978 *Electrical breakdowns of gases* (New York: Wiley)
- [21] Nevshupa R A and Nakayama K *Vacuum*
- [22] Matsunuma S and Hosoe Y 1997 *Tribology Int.* **30** 121
- [23] *The Asahi-shimbun* 4 August 2001 p 31 [in Japanese]